2742–2755 Nucleic Acids Research, 2011, Vol. 39, No. 7 Published online 24 November 2010
doi:10.1093/nar/gkq1191

Regulation by interdomain communication of a headful packaging nuclease from bacteriophage T4

Manjira Ghosh-Kumar[1], Tanfis I. Alam[1], Bonnie Draper[1], John D. Stack[2] and Venigalla B. Rao[1,*]

[1]Department of Biology, The Catholic University of America, Washington, DC 20064 and [2]Department of Physics and Beckman Institute, University of Illinois at Urbana-Champaign, Urbana, IL 61801, USA

Received September 22, 2010; Revised November 3, 2010; Accepted November 4, 2010

ABSTRACT

In genome packaging by tailed bacteriophages and herpesviruses, a concatemeric DNA is cut and inserted into an empty procapsid. A series of cuts follow the encapsidation of each unit-length 'headful' genome, but the mechanisms by which cutting is coupled to packaging are not understood. Here we report the first biochemical characterization of a headful nuclease from bacteriophage T4. Our results show that the T4 nuclease, which resides in the C-terminal domain of large 'terminase' gp17, is a weak endonuclease and regulated by a variety of factors; Mg, NaCl, ATP, small terminase gp16 and N-terminal ATPase domain. The small terminase, which stimulates gp17-ATPase, also stimulates nuclease in the presence of ATP but inhibits in the absence of ATP suggesting interdomain crosstalk. Comparison of the 'relaxed' and 'tensed' states of the motor show that a number of basic residues lining the nuclease groove are positioned to interact with DNA in the tensed state but change their positions in the relaxed state. These results suggest that conformational changes in the ATPase center remodel the nuclease center via an interdomain 'communication track'. This might be a common regulatory mechanism for coupling DNA cutting to DNA packaging among the headful packaging nucleases from dsDNA viruses.

INTRODUCTION

The double-stranded DNA bacteriophages are widely distributed in nature and likely form the largest biomass on the planet (1). These and a large group of eukaryotic viruses such as herpes viruses have similar life cycles and process genomes by common mechanisms. The newly replicated viral genome is a concatemer, a head to tail polymer of the viral genome. The phage T4 concatemer is a complex structure consisting of many branches arising due to recombination-dependent DNA replication (2,3). The phage 'terminase' complex, a hetero-oligomer of small and large terminase subunits, recognizes the viral genome, makes an endonucleolytic cut and inserts the end into an empty prohead by docking at the special portal vertex of the prohead (4). A packaging motor powered by an ATPase present in the large terminase (5,6) translocates DNA into the prohead. When the head is full ('headful' packaging) the DNA is cut, separating the packaged head from the terminase-concatemer complex. The latter then docks onto another empty prohead and continues the encapsidation process. Neck and tail proteins assemble on the portal of the DNA-full head and complete the assembly of an infectious virion.

Viral genome processing must be tightly regulated such that each capsid receives one contiguous stretch of viral DNA that is equivalent to one (e.g. phage λ) or slightly more than one (e.g. phage T4) genome length in order to produce an infectious virus (4). First, it should be coordinated with other DNA metabolic pathways, e.g. recombination and repair, such that branches are resolved and a linear dsDNA is continuously 'fed' to the packaging machine. Second, the initial cut must occur rarely and in conjunction with packaging initiation such that the viral genome is not fragmented prior to encapsidation. Third, the termination cut must be coupled to headful DNA packaging so that a full-length viral genome is encapsidated without any cutting during translocation. These steps must occur with precision in order to sustain a fast packaging motor that can translocate up to ~2000 bp/s (7).

In *cos* phages such as λ, the terminase makes the first cut at a unique sequence, *cos*N, translocates one unit length genome, and then makes the second cut at the

*To whom correspondence should be addressed. Tel/Fax: +1 202 319 5721; Email: rao@cua.edu

The authors wish it to be known that, in their opinion, the first two authors should be regarded as joint First Authors.

© The Author(s) 2010. Published by Oxford University Press.
This is an Open Access article distributed under the terms of the Creative Commons Attribution Non-Commercial License (http://creativecommons.org/licenses/by-nc/2.5), which permits unrestricted non-commercial use, distribution, and reproduction in any medium, provided the original work is properly cited.

next *cos*N sequence that is ~45 kb distance from the first cut (8,9). In *pac* phages such as P22 and SPP1, the very first cut is made near a *pac* site but the second and subsequent cuts are made at a random sequence after ~104–110% genome length DNA is packaged (10–12). Phage T4 is similar to *pac* phages except that even the first cut does not strictly occur near a unique *pac* sequence, however, there is evidence for at least one *pac* site near gene 16 (13,14). Regardless of the differences in sequence specificity, the spacing between the cuts is equivalent to one headful or one genome length of the respective virus.

The T4 terminase complex consists of the small terminase subunit, gp16 (18 kDa) and the large terminase subunit, gp17 (70 kDa) (15) ('terminase' and 'terminase subunit' are interchangeably used). gp17 consists of two domains, the N-terminal ATPase domain that provides energy for DNA translocation (16,17) and the C-terminal nuclease domain that makes the packaging initiation and termination cuts (18–20). X-ray structures show that the ATPase domain consists of subdomain I, a six-stranded parallel β-sheet that is typically found in RecA-type ATPases and subdomain II that is connected to the nuclease domain via flexible linker or hinge (21,22). Subdomain I contains the signature motifs such as Walker A, Walker B and catalytic carboxylate, whereas subdomain II is a 'transmission' domain that regulates the hydrolysis of ATP bound in the cleft formed by the two subdomains. The nuclease domain has an RNase H fold that is found in RNase Hs, resolvases and integrases, and contains Mg-coordinated catalytic center formed by a triad of acidic residues, Asp401, Asp542 and Glu458 (23,24). A structurally well conserved C-terminal nuclease domain has also been found in phage SPP1 (G2P) and herpesvirus 5 (UL-89) large terminases (24,25). The C-domain shows two putative DNA binding grooves, one for DNA cleavage and another for DNA translocation (22). The small terminase gp16 does not possess any of these motifs or activities but regulates the activities of the large terminase (26).

Cryo-EM reconstruction of the packaging machine shows a ring of five gp17 molecules assembled on the prohead portal into a pentameric motor with the translocation groove facing the channel and the nuclease groove facing away from the channel (22). An electrostatic force driven translocation mechanism was proposed in which gp17 alternates between two conformational states, a tensed state in which the domains come into close contact through complementary charged pair interactions and a relaxed state in which the domains are separated by ~7 Å. The C-domain-bound DNA is translocated into the capsid by 2 bp when gp17 changes its conformation from relaxed to tensed state. The domain movements are facilitated by an interdomain linker or hinge that connects the ATPase subdomain II to the C-domain (22).

Although the structural and functional motifs involved in DNA translocation have been well characterized, the mechanisms of DNA cutting and its regulation by packaging remained poorly understood. The T4 system is particularly intriguing because despite lacking sequence specificity, the efficiency of infectious virion production is one of the highest, approaching the theoretical efficiency of 1 (27). Here we report the first biochemical characterization of gp17 nuclease, which provides insights into the catalysis and regulation of headful packaging nucleases. Our results show that the gp17 nuclease is a catalytically weak endonuclease and its activity is highly regulated. The enzyme is optimally active at low Mg or NaCl concentrations but inhibited at high (physiological) concentrations. Under conditions of high turnover of ATP hydrolysis, when gp16, gp17 and ATP are present, the nuclease is stimulated, but inhibited in the absence of ATP. Structural analyses show that in the tensed state, a number of basic residues lining the nuclease groove are correctly positioned to interact with the bound DNA, whereas in the relaxed state, the residues are predicted to be out of position. These results suggest that conformational changes in the ATPase center remodel the nuclease center. An interdomain communication track consisting of residues from subdomain II, hinge and β-hairpin apparently relays conformational signals elicited by regulators, favoring either the nuclease active state or the inactive state. This might be a novel regulatory mechanism for coupling DNA cutting to headful packaging by dsDNA viruses.

MATERIALS AND METHODS

Protein purification

The pET-15b and pET-28b plasmid constructs containing inserts for gp16, gp17 (K577, amino acids 1–577; C360, amino acids 360–577 or RB49-C360, amino acids 360–607) were transformed into *Escherichia coli* BL21 (DE3) pLys-S cells. Recombinant cells were grown to log phase at 30°C in Moore/amp/chl medium (2% tryptone, 1.5% yeast extract, 0.2% Dextrose, 0.8% NaCl, 0.2% Na_2HPO_4 0.1% KH_2PO_4, 100 mg/l ampicillin and 34 mg/l chloramphenicol). IPTG (1 mM) was added to induce over-expression of the recombinant protein. The cells were pelleted and resuspended in 20 ml binding buffer A [20 mM Tris–HCl pH 8, 1 mM ATP, 5 mM Mg^{2+}, 100 mM NaCl, 10 mM imidazole and protease inhibitor cocktail (Roche)]. The cells were lysed by French Press and the supernatant was applied to Histrap column (AKTA-Prime, GE Healthcare). The hexa-His tagged protein was eluted using a gradient of 50–500 mM imidazole and the peak fractions were applied to Mono-Q HR column pre-equlibrated with buffer B (20 mM Tris–HCl pH 8, 30 mM NaCl). The protein was eluted using 30–500 mM NaCl gradient in buffer B. The peak fractions were applied to Superdex-200 gel filtration column pre-equilibrated with buffer C (20 mM Tris–HCl pH 8, 100 mM NaCl). The peak fractions were applied to single-stranded DNA-cellulose column pre-equilibrated with buffer B containing 1 mM EDTA to absorb any contaminating nucleases. The flow-through fractions were concentrated and stored at −80°C.

In vitro nuclease assay

The purified gp17 and gp16 (concentrations as indicated in the figures or legends to figures) were incubated with plasmid DNA [pAd10, 29 kb (28); pUC19, 2.7 kb; pET-28b, 5.3 kb] in a reaction mixture of 25 µl containing 4 mM Tris–HCl, pH 8, 5 mM $MgCl_2$ and 6 mM NaCl for 15 min at 37°C. In most experiments, gp17-K577 (amino acids 1–577) in which the C-terminal 33 amino acids were deleted was used. gp17-K577 retained all the known enzymatic functions of the full-length protein but it is protease-resistant during purification and migrates as a single band by SDS–PAGE. The activity was terminated by adding EDTA to 50 mM final concentration and analyzed by electrophoresis on 0.8% (w/v) agarose gel followed by ethidium bromide staining.

To analyze size preference for DNA substrate, gp17 (3 µM) or DNase I (0.004 µM) (Sigma) was incubated with ^{32}P-labeled λ DNA-HindIII marker (120 ng) (Promega) in the presence of AMP-PNP in a 25 µl reaction mixture. The λ DNA-HindIII marker was pre-incubated at 55°C for 5 min and immediately cooled on ice to 'melt' any reannealed *cos*-containing 23 and 4 kb DNA fragments. The reactions were stopped by the addition of EDTA and the gp17-digested DNA was separated by 0.8% agarose gel (w/v) electrophoresis (DNA ladder; New England Biolabs) or 4–20% PAGE (λ DNA-HindIII, Invitrogen). The ^{32}Pi-labeled DNA fragments were quantified by Phosphorimaging (Storm 820, Molecular dynamics).

To prepare circular relaxed pUC19 and pET-28b, the plasmids (5 µg) were treated with DNA topoisomerase-I (New England Biolabs) in a 25 µl reaction mixture at 37°C for 1h.

DNA ligase assay

Circular pUC19 DNA (40 ng) was cleaved with gp17 (as described above) or BamHI. The digested DNA was precipitated by 8 M ammonium acetate and resuspended in water, followed by the addition of T4 DNA ligase (Fermentas) or *E. coli* DNA ligase (New England Biolabs) in a 25 µl reaction mixture. The samples were incubated at 16°C for 16 h and analyzed by agarose gel electrophoresis.

Molecular dynamics simulations

The full-length (amino acids 10–562) relaxed structure was constructed from 2O0H.pdb (amino acids 10–357) and 3CPE.pdb (amino acids 358–562), solvated in a water box neutralized with Na and Cl ions, and a short (20ps) equilibration simulation was run using NAMD (29) at 300 K. The resulting monomer was replicated five times, reconstructed as an initial model of a relaxed pentameric gp17 motor and neutralized in a $180 \times 185 \times 110$ Å water box, giving the motor ~30Å of padding with water in all directions. Molecular dynamics flexible fit (30) runs were performed using the relaxed initial gp17 model constructed above and the trimmed cryo-EM map of the T4 procapsid-gp17 complex (EMD-1572). The MDFF runs were stopped when the rmsd of the fitted gp17 compared to the initial configuration had stabilized.

Modeling and normal mode analyses

The unresolved region of RB49 nuclease (amino acids 523–535) and the T4 nuclease (amino acids 361–567) were modeled from the RB49 template (PDB ID: 3C6A) using SWISS-MODEL (http://swissmodel.expasy.org/) with default parameters. The T4 nuclease model or the full length T4 gp17 (PDB ID: 3CPE) was uploaded to the El Nemo Elastic Network Model Server (http://igs-server.cnrs-mrs.fr/elnemo/) and normal mode analysis was performed with default parameters. Images and movies were created with PyMol (http://www.pymol.org/).

RESULTS

The gp17 large terminase is a weak endonuclease

Previous studies established that gp17, either the over-expressed protein in *E. coli* or a highly purified protein *in vitro*, non-specifically cleaves DNA producing a smear of fragments (18,19,20,23).

Two pieces of evidence indicated that gp17 is an endonuclease that makes double-stranded cuts in DNA: (i) the time course of pET28b plasmid cleavage showed that the linear DNA appears at the earliest time point (30 s; Figure 1A, lane 2) and accumulates with increasing time. The linear DNA is then degraded to a smear of DNA fragments (lanes 9–12; also see panel C, lanes 9–14). However, a small amount of nicked relaxed DNA is seen (lanes 3–6) indicating that the enzyme may also have a low level of single-stranded nickase activity. Secondly, gp17 cleaved the topoisomerase I relaxed DNA as efficiently as the supercoiled DNA (Figure 1B; data not shown) suggesting that single-stranded regions that are part of cruciform structures, which are generally present in the supercoiled DNA, are not essential for cutting.

To determine its catalytic capacity relative to other nucleases, the activity of gp17 nuclease was compared to that of pancreatic DNase I, a non-specific nickase and Sau3AI, a frequent cutting restriction endonuclease. As shown in Figure 1C, the circular DNA was first cleaved to the linear form (lanes 4–8) and then further digested to small fragments (lanes 9–14). At low gp17 concentrations (lanes 4–7), some of the DNA was retained in the well, which probably represents a reaction intermediate, DNA-substrate complex, as this material was also stained with Coomassie blue (data not shown). The enzyme:DNA ratio for 50% cleavage was approximately 270 for gp17, which was approximately 370 times greater than that of Sau3AI and approximately 9000 times greater than that of DNase I (Figure 1D). These data suggest that gp17 is a weak endonuclease.

gp17 nuclease prefers long DNA substrates

gp17 nuclease showed proportionally greater activity with increasing DNA length. About four times fewer gp17 molecules are required to cleave the 29 kb pAd10 plasmid

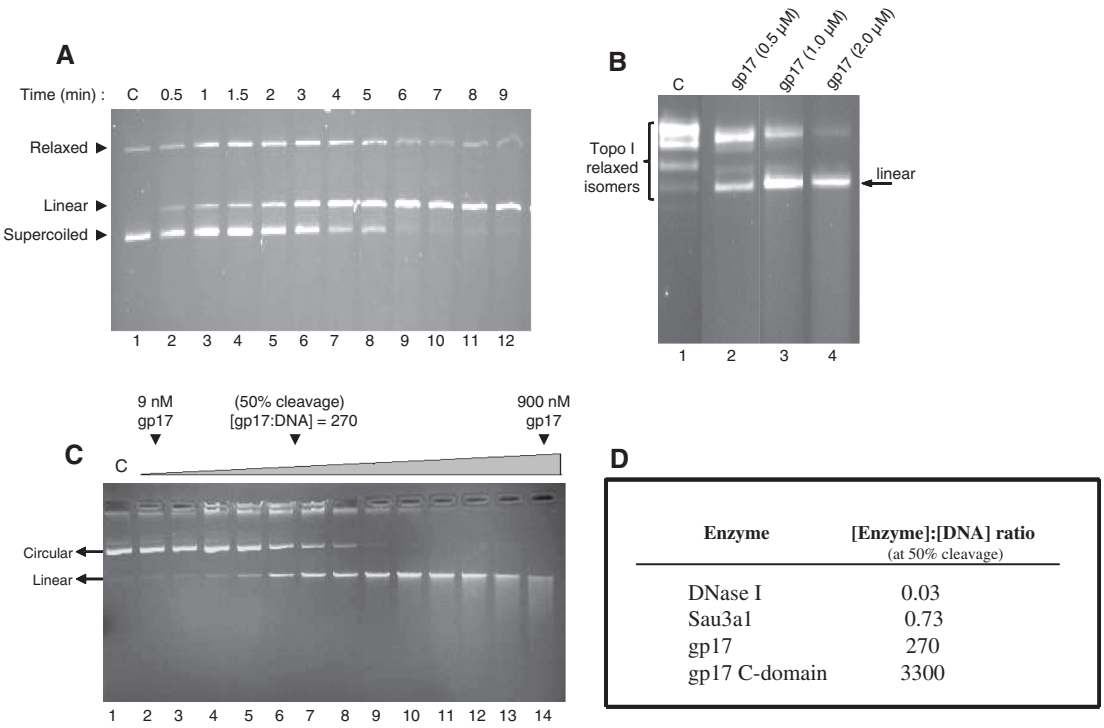

Enzyme	[Enzyme]:[DNA] ratio (at 50% cleavage)
DNase I	0.03
Sau3a1	0.73
gp17	270
gp17 C-domain	3300

Figure 1. The large terminase gp17 is a weak endonuclease. (**A**) Time course of cleavage of circular pET28b plasmid (100 ng) by gp17 (1.5 μM). (**B**) Cleavage of topoisomerase I relaxed DNA by gp17. (**C**) Increasing concentrations of gp17 (9–900 nM) were incubated with circular pAd10 DNA (400 ng, 0.9 nM) and the amount of undigested circular DNA in each lane was quantified by laser densitometry. (**D**) Comparison of the nuclease activity of T4 gp17 with DNase I (non-specific nickase) and Sau3A1 (frequent cutting restriction endonuclease). Increasing concentrations of each enzyme were incubated with circular pAd10 DNA (400 ng, 0.9 nM) with the enzyme (monomer) to DNA ratio (number of molecules of each) varied over a range of 10–1000:1. The enzyme:DNA ratio at 50% cleavage was determined by quantifying the amount of undigested circular DNA in each lane. Values represent average of duplicates from two independent experiments. The 'C' lanes represent untreated DNA. See 'Materials and Methods' section for additional details.

DNA when compared to the 2.6 kb pUC19 DNA (Figure 2A). When a ladder of DNA fragments was used as a substrate (Figure 2B), large fragments such as the 10 kb DNA were completely digested by 5 min (lane 3) whereas a significant portion of the short fragments in the range of 0.5–1 kb remained intact even after 30 min incubation (lane 7). This is also clearly evident with the ^{32}P-end labeled λ-HindIII fragments in which various length fragments are present at equimolar concentration. Cleavage rate was proportional to the length of the DNA fragment, with the 23 kb DNA being the fastest digested fragment [Figure 2C, lanes 2–6)]. DNase I on the other hand digested all the DNA fragments at the earliest time point showing no size preference (lanes 7–11).

gp17 nuclease preferentially cleaves at the ends of linear DNA

Since gp17 preferentially packages from ends of linear DNA (31,32), we hypothesized that gp17 may preferentially bind to and cut near the end. This was tested by analyzing the size of the fragments produced when gp17 cleaves ^{32}P-end labeled λ-HindIII DNA fragments. If cleavage occurred preferentially near the end, short ^{32}P-labeled fragments would be produced. Otherwise, the cleaved ^{32}P-products will have a random length distribution and migrate as a smear throughout the lane. As shown in Figure 2C, even at 2 min incubation, most of the radioactivity appeared near the bottom of the gel (lane 2), suggesting that gp17 preferentially cuts near the ends. On the other hand, DNase I that randomly nicks DNA produced broad smears throughout the lane (lanes 7–11).

gp17 nuclease produces blunt ends

To determine if gp17 makes blunt cuts or staggered cuts, the gp17-digested fragments were ligated with *E. coli* and T4 DNA ligases (Figure 2D). Both the enzymes can ligate 'sticky' ends but only the T4 ligase can ligate blunt ends. The data showed that only the T4 ligase (lane 4), but not the *E. coli* ligase (lane 3), could ligate the gp17-cleaved pUC19 DNA or pAd10 DNA (data not shown) producing high molecular weight products. This agrees with a previous report showing that the mature phage T4 DNA can be ligated with T4 DNA ligase (33).

Metal ion specificity of gp17 nuclease

The gp17 nuclease domain has an RNase H fold and it was hypothesized that gp17, like the RNase H, requires two Mg ions for catalysis (23,34,35). In fact, one or two Mg ions are present in the catalytic site of gp17, SPP1 and herpesvirus nuclease domain crystal structures (22,24,25). The metal ion requirement was tested with different metal ions and at different concentrations of $MgCl_2$. gp17 showed no significant cleavage in the absence of Mg but

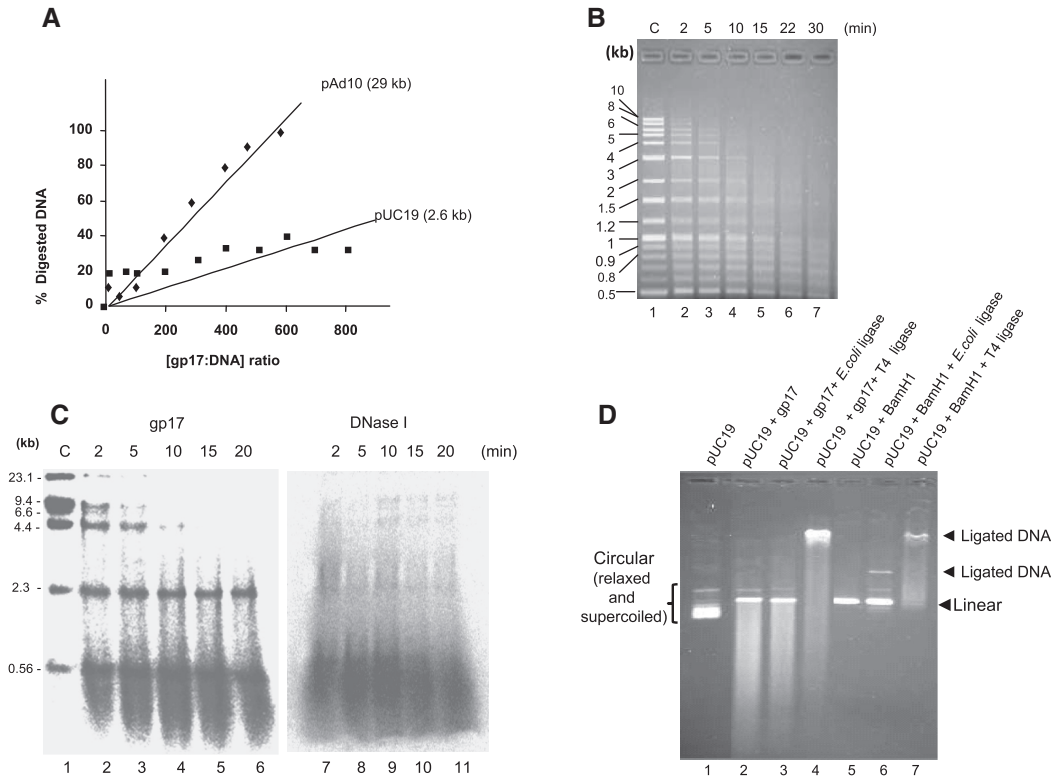

Figure 2. gp17 nuclease prefers long DNA substrates and cleaves at the ends of linear DNA. (**A**) Increasing concentrations of gp17 were incubated with 0.9 nM each of 29 kb pAd10 plasmid DNA or 2.6 kb pUC19 plasmid DNA. The undigested circular DNA was quantified and used to determine the percent of cleaved DNA at different gp17:DNA ratios. Values represent the average of duplicates from two independent experiments. (**B**) gp17 preference for longer DNA molecules was seen by incubating gp17 (3 μM, lanes 2–7) with a 2-log DNA ladder (400 ng, 0.1–10 kb, New England Biolabs) for 2–30 min. (**C**) Autoradiogram showing the cleavage of γ^{32}P end-labeled λ-HindIII DNA fragments (0.5 pmol, 125–23 130 bp, Promega) by gp17 (1.2 μM) (lanes 2–6) or DNase I (0.0024 μM, 500-fold less than gp17) (lanes 7–11). Lane 1 has untreated DNA. (**D**) gp17 nuclease generates blunt ends. Circular pUC19 DNA (40 ng) was cleaved by gp17 (lanes 2–4) or BamH1 (lanes 5–7). The cleaved DNA was then treated with *E. coli* DNA ligase (lanes 3 and 6) or T4 DNA ligase (lanes 4 and 7). Lanes labeled as 'C' are control untreated lanes. See 'Materials and Methods' section for additional details.

remains tightly bound to DNA, as evident by the shift of DNA to the well (Figure 3A, lane 2). Cleavage was maximal at low Mg concentrations (1–2 mM), essentially degrading all DNA to low molecular weight products (lanes 3 and 4 where the DNA smear is barely visible). The activity then decreased with increasing $MgCl_2$ concentration eventually stopping after the 'first cut', conversion of circular to linear DNA, is made (lanes 10–12). Mn can substitute for Mg, showing even better activity than Mg (Figure 3B, lane 5 with Mn showing complete degradation when compared to lane 3 with Mg). However, none of the other ions tested, Ca^{2+}, Zn^{2+}, Ni^{2+} or Co^{2+}, showed significant cleavage (Figure 3B, lanes 4 and 6–8). These data suggest that gp17 has stringent metal ion requirement, presumably because the metal ion must precisely fit into the catalytic pocket in order to coordinate with the catalytic triad acidic residues (36).

gp17 nuclease is highly sensitive to salt

gp17 nuclease activity is the highest at a low sodium chloride concentration (6 mM) (Figure 3C, lanes 2 and 9) and the activity decreases with increasing concentrations (lanes 3–7 and 10–14). At ~60 mM or greater, including the physiological concentration (150 mM), the activity is nearly completely inhibited. The same pattern was observed whether the substrate is linear DNA (lanes 1–7) or circular DNA (lanes 8–14). But once again, the first cut that converts circular DNA to linear DNA is insensitive to high salt (lanes 10–14, in particular lane 14 where all the circular DNA is converted to linear form even at 150 mM NaCl).

ATP stimulates gp17 nuclease

gp17 nuclease activity is stimulated by ATP (Figure 4A). In the presence of 1 mM ATP, the DNA is completely digested to very short oligonucleotides (see the DNA band below the dye band in Figure 4B, lane 3). The non-hydrolyzable analogs, ATPγs and AMP-PNP, also showed stimulation but considerably lower than ATP (Figure 4B, lanes 5 and 6), but the product, ADP, showed no significant stimulation and may in fact have a slight inhibitory effect (Figure 4B, lane 4), suggesting that the nucleotide state of gp17 affects DNA cutting. Although there is some inhibition at high ATP concentrations (e.g. 5 mM ATP; Figure 4A, lane 11), unlike Mg^{2+} and NaCl (Figure 3), cutting was not restricted to the first cut.

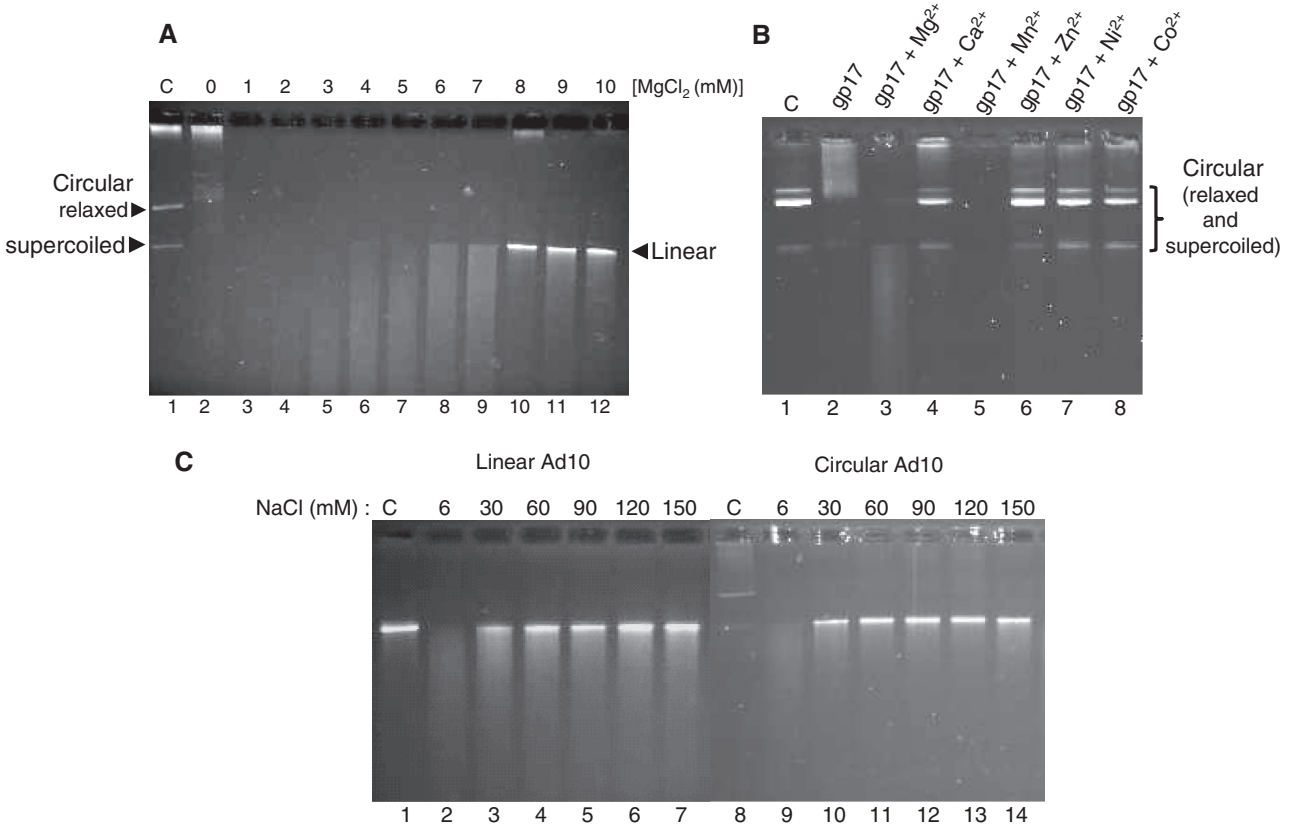

Figure 3. Metal ion specificity and salt sensitivity of gp17 nuclease. (**A**) gp17 (1.2 μM) was incubated with circular pAd10 DNA (100 ng) in the presence of 1–10 mM $MgCl_2$. (**B**) gp17 (1.2 μM) was incubated with circular pAd10 DNA (100 ng) containing no metal ion (lane 2) or 1 mM of $MgCl_2$, $MnCl_2$, $CaCl_2$, $ZnCl_2$, $NiCl_2$ or $CoCl_2$. (**C**) gp17 (2 μM) was incubated with linear pAd10 DNA (lanes 2–7) or circular pAd10 DNA (lanes 9–14) in the presence of 6–150 mM NaCl. Lanes 'C' are control lanes showing untreated DNA.

Nucleotide state of ATPase domain affects nuclease activity

ATP stimulation implies that there is communication between the N-terminal ATPase domain and the C-terminal nuclease domain because the ATP binding site is present in the N-terminal domain. However, the presence of a cryptic ATP binding site in the C-domain cannot be excluded. In fact, phage lambda gpA large terminase is reported to have an ATPase site in the C-domain, in addition to the one in the N-domain (37). To analyze this question, the effect of ATP was tested using the purified gp17 C-domains from phages T4 and RB49. The RB49 C-domain was included in this experiment because it, unlike the T4 C-domain, exhibited greater nuclease activity. Unlike the stimulation observed with full-length gp17, no significant ATP stimulation was observed with the C-domains (Figure 4C). ATP analogs, ATPγs and AMP-PNP, also did not show any stimulation (data not shown). These results suggest that interaction of the nucleotide at the N-terminal ATPase center affects nuclease activity of the C-domain.

gp16 interaction with the ATPase domain modulates nuclease activity

Previously we have shown that gp16 inhibits gp17 nuclease activity (26). At ~6:1 molar ratio of gp16 to gp17 [or ~1:1 ratio of gp16 oligomer (presumed octamer) to gp17 monomer], cutting of linear DNA is almost completely inhibited, but as in the case of Mn and NaCl, the first cut is 'immune' to inhibition (Figure 5A). Unexpectedly, in the presence of ATP, gp16 has an opposite effect, stimulation of gp17 nuclease. This is most obvious at low gp17 concentrations, e.g. 0.25 and 0.5 μM gp17, where cutting is otherwise negligible in the absence of gp16 [Figure 5B; compare lanes 2 and 3 (without gp16) with lanes 7 and 8 (with gp16)]. The non-hydrolyzable analog AMP-PNP did not show as high stimulation under the same conditions (compare lanes 7 and 8 of Figure 5C with those of Figure 5B). These results show that gp16 regulates nuclease activity, stimulating in the presence of ATP (stimulated ATPase causing high turnover of ATP hydrolysis; 5) and inhibiting in the absence of ATP.

Nuclease cutting is restricted to the first cut in the presence of all regulators

As described above, at physiological salt concentration (150 mM NaCl), gp17 nuclease can efficiently make the first cut (Figure 3C). The same was observed even under conditions where gp17 nuclease is stimulated the most, in the presence of both gp16 and ATP. As shown in Figure 5D (lanes 2 and 3), gp17 cleaved DNA into small

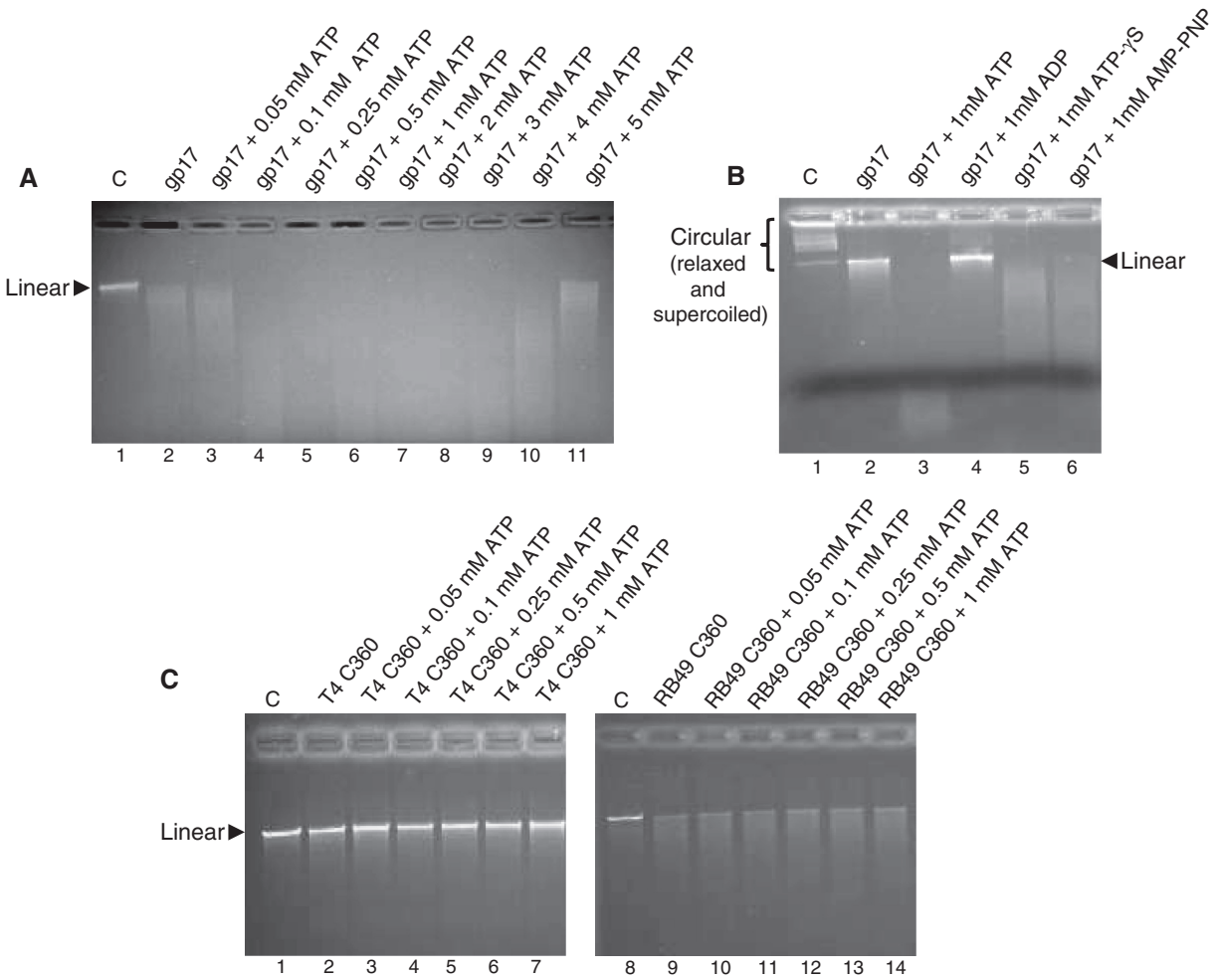

Figure 4. ATP stimulates gp17 nuclease. (**A**) Nuclease activity of gp17 is stimulated in presence of ATP. gp17 (1 μM) was incubated with linear pAd10 DNA (100 ng) in the presence of increasing concentrations of ATP (0.05–5 mM). Note that the DNA is degraded to small fragments in some of the lanes. Therefore, very little DNA smear is seen in these lanes. (**B**) Nuclease activity of gp17 in the presence of ATP analogs. gp17 (1.2 μM) was incubated with circular pAd10 DNA (200 ng) in the presence of ATP, ADP, ATP-γS or AMP-PNP (1 mM). (**C**) The T4 nuclease domain (C360, amino acids 360–577) (left panel; lanes 1–7) or the RB49 nuclease domain (C360, amino acids 358–607) (right panel; lanes 8–14) is not stimulated by ATP. T4 C360 (4 μM) or RB49 C360 (1 μM), either alone (lanes 2 and 9) or in the presence of ATP (lanes 3–7 and 10–14) was incubated with linear pAd10 DNA (100 ng) for 15 min and the samples were analyzed by 0.8% (w/v) agarose gel electrophoresis. Lanes 1 and 8 labeled as 'C' are control lanes having untreated DNA.

fragments in the presence of gp16 and ATP but was restricted to only the first cut in the presence of NaCl (lanes 4–7). A slightly higher concentration of salt (60 mM) was required to completely inhibit the gp17 nuclease stimulated by both gp16 and ATP (lane 4) when compared to that stimulated by ATP alone (30 mM) (lane 9). Similar results were obtained when different plasmid DNAs such as pET28b and pUC19 were used as substrates (data not shown).

Tensed and relaxed conformational states might represent active and inactive states of nuclease

The X-ray structure of the packaging motor shows that gp17 adopts a tensed state (supposed to be ATP-bound) (Figure 6A) whereas cryo-EM reconstructions show a relaxed state (apo) suggesting that gp17 alternates between the two states, powering DNA into the capsid (22). We have constructed a pseudoatomic model for the relaxed state using molecular dynamics simulations (Figure 6A; see 'Materials and Methods' section for details). Relaxed gp17 monomers were first constructed using the N-domain of a relaxed crystal structure [2O0H.pdb, (21)] connected to the C-domain crystal structure [3CPE.pdb (22); the crystal structure and the key catalytic residues of the RB49 C-domain (3C6A.pdb) are very similar to those of the T4 C-domain in the tensed structure (Supplementary Figure S1)]. Combining these into a pentamer, the hybrid model was then fitted to the gp17 portion of the cryo-EM map. The output of this fitting process gave a set of atomic coordinates characteristic of the relaxed state. It is worth noting that two features of the ATPase domain found in previous work can be seen here in detail. Namely, comparing tensed and relaxed monomers with N subdomains I aligned, there is a relative rotation of N subdomain II by several degrees. Second, if N-domains of relaxed and tensed monomers

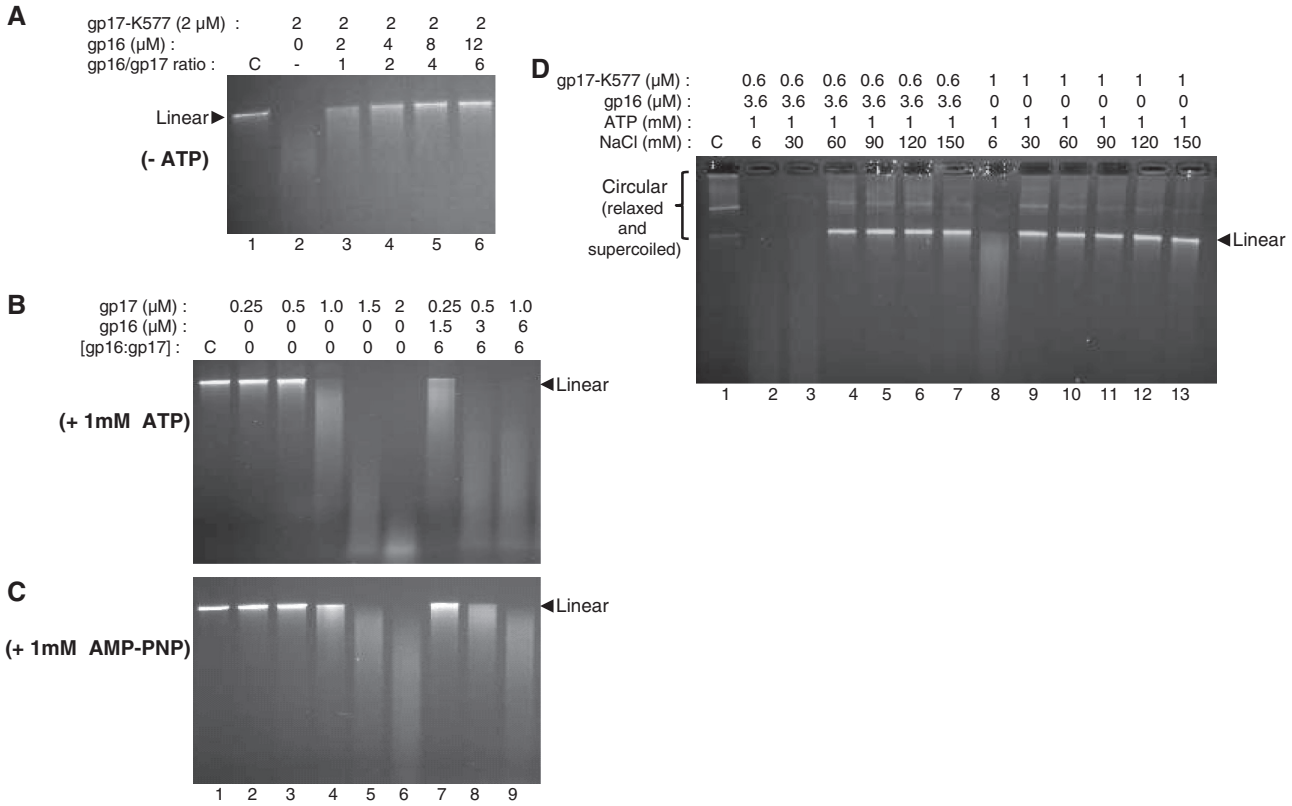

Figure 5. The small terminase, gp16, regulates gp17 nuclease activity. gp17 alone or in the presence of gp16 at different molar ratios of gp16:gp17 was incubated with linear pAd10 DNA (100 ng) and no nucleotide (**A**), 1 mM ATP (**B**) or 1 mM AMP-PNP (**C**) for 15 min. (**D**) gp17 (0.6 or 1 μM) was incubated with ATP (1 mM), either without gp16 (lanes 8–13) or with gp16 at a gp16:gp17 molar ratio of 6 (lanes 2–7), and increasing concentration of NaCl (6–150 mM). Lanes labeled as 'C' are control untreated DNA. See 'Materials and Methods' section for additional details.

are aligned, the C-domains are separated by several angstroms, of which ~7Å is in the vertical direction. Both of these motions are thought to be important in DNA translocation (Figure 6A).

Comparison of the tensed (X-ray structure) and relaxed (MD simulation) monomers showed that the positions of several interdomain residues shifted significantly. Figure 6B plots the distance moved by backbone atoms from the tensed to the relaxed state after C-domain alignment and backbone *rmsd* minimization. The most significant difference occurs for residues in the hinge (residues 354–364) and the β-hairpin (residues 525–535), which is expected considering that these are known [hinge (22)] or predicted [β-hairpin (24)] to be flexible regions. While the flexible hinge has few packing constraints in either state, the β-hairpin moves away from the nuclease groove and forms new contacts with the ATPase subdomains I and II in the relaxed state (Figure 7A and B).

The next largest motions occur for residues near either R406 or the charged patch containing residues K490, K493, R494 and K496, a snapshot of which is shown in Figure 6C. These residues are likely important for positioning DNA in the nuclease groove prior to cutting (22; M. Ghosh-Kumar and V.B. Rao, unpublished results). The backbone positions of these residues shift, narrowing the DNA binding groove from ~21–23Å in the tensed state to ~17–19Å in the relaxed state (Figures 7C and D). In the tensed state, the phosphate groups of DNA modeled in the groove (Figure 7C) align with the basic residues; but in the relaxed state, these residues are not positioned to interact with DNA in the same way. Thus the nuclease DNA binding groove appears to be 'remodeled' when gp17 switches conformation between tensed and relaxed states, tensed state being nuclease-active and relaxed state being nuclease-inactive.

DISCUSSION

Most tailed bacteriophages and herpes viruses replicate their genomes as a concatemer, which in T4 is a highly branched, endless, structure. Genome processing requires that an end be created first by an endonucleolytic cut and inserted into the prohead to initiate packaging. After encapsidation of one, or slightly more than one, (headful) viral genome, a second cut is made to terminate packaging. Cutting must be coordinated such that a single cut is made at the very beginning of the process, followed by a series of cuts each coupled to headful packaging. Otherwise, indiscriminate random cutting would lead to fragmentation of genome and would be suicidal to the virus. Recent biochemical and structural studies show that a nuclease catalytic center in the C-terminal domain of phage T4 large terminase gp17 is responsible for these cuts (20,22,23). But the mechanism

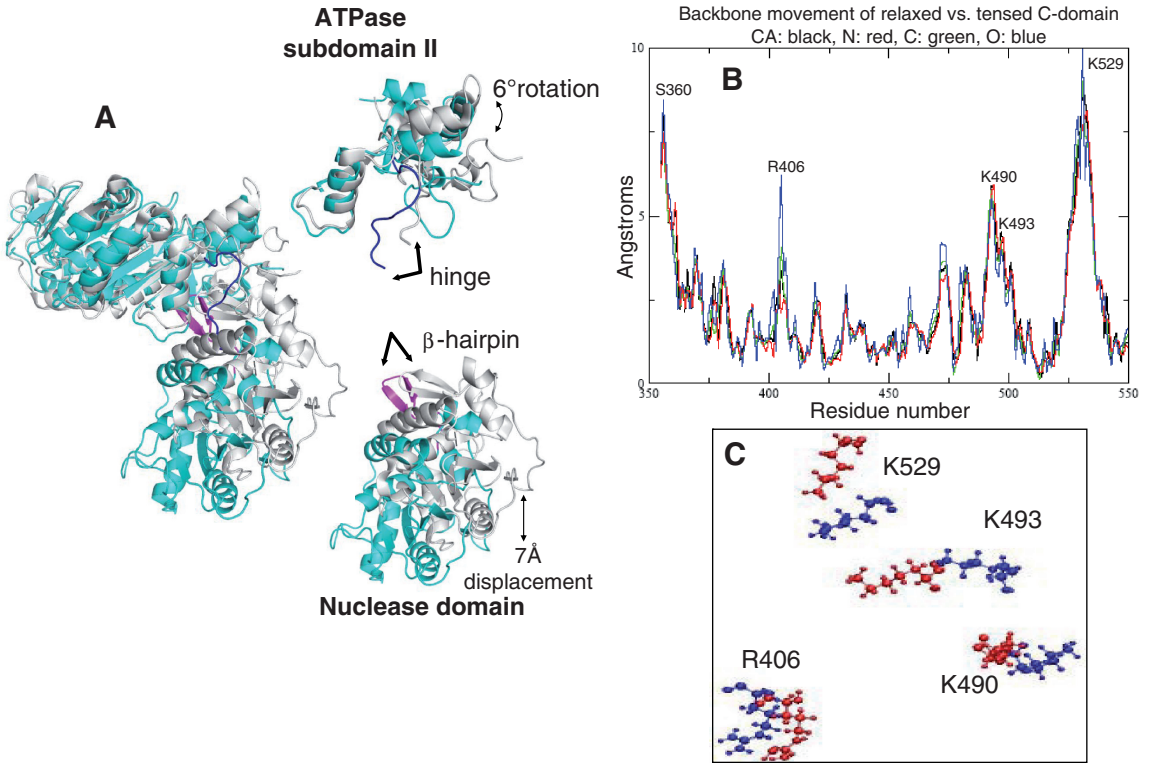

Figure 6. Conformational switching from tensed state to relaxed state alters the nuclease DNA groove. (**A**) gp17 in the tensed state (PDB ID: 3CPE, gray) is superimposed with the relaxed state (cyan) constructed by molecular dynamics simulations (see 'Results' and 'Materials and Methods' sections for details). Comparing the two states shows ~6° rotation of ATPase subdomain II and ~7Å displacement of the nuclease domain. In addition, the flexible interdomain hinge (dark blue line) and the β-hairpin (magenta) show significant movement. (**B**) Distances between backbone atoms of tensed and relaxed C-domains, after minimizing overall rmsd backbone between the two. (**C**) Comparison of location of basic residues lining the DNA binding groove (relaxed: red, tensed: blue).

by which cutting and packaging are coupled remained unknown. Here we report the first biochemical characterization of a headful packaging nuclease from phage T4, which suggests novel mechanisms of regulation in dsDNA viruses.

The enzymatic properties of gp17 nuclease are consistent with its role as a packaging nuclease. First, gp17 is a very weak endonuclease. Merely making a single cut required a gp17: DNA molar ratio of approximately 500. Second, once a cut is made, the enzyme seems to attach to the end and makes additional cuts near the end rather than randomly cutting elsewhere in the DNA. These features, and the fact that gp17 levels in the infected cell are extremely low (38), mean that gp17 at best can only make infrequent cuts in the viral genome. Third, the gp17 nuclease preferentially cleaves longer DNA substrates. When equimolar amounts of various size linear DNA fragments are added to the reaction mixture, the longest DNA fragment (>10 kb) is cleaved the fastest and the small fragments, ≤2 kb in size, remained relatively intact even after a long incubation time. These results indicate that cutting might require interaction between at least two gp17 molecules bound at different sites on the same DNA, probably as an anti-parallel dimer, as the latter is a requirement for cutting by dsDNA endonucleases (39,40). The longer the DNA, the greater the probability of forming such a complex by looping out the DNA flanking the bound gp17 molecules. With short DNAs, not only would the probability be low but also that there might be a greater energy cost for looping or bending DNA, thus the greatly reduced cleavage. In fact, DNA looping/bending might be a common mechanism for packaging initiation cuts, as has been well documented in phage λ where the terminase uses the assistance of the *E. coli* integration host factor (IHF) to form a bent DNA-terminase complex (41,42). This feature has also been well documented in the analogous type-I restriction enzyme translocases, which form stable anti-parallel dimers by diffusible DNA looping (43).

Our results show that the phage T4 packaging nuclease is one of the most regulated nucleases reported to date. Many components: Mg, NaCl, ATP, N-terminal ATPase domain and small terminase gp16 influence gp17 nuclease activity. An optimal concentration of Mg (or Mn) (1–2 mM) or NaCl (6 mM) is required for efficient cleavage, but higher than optimal concentrations, notably physiological concentration of salt (150 mM), results in near complete inhibition of cutting. Strikingly however, the 'first cut', conversion of circular to linear DNA, is immune to this inhibition. We hypothesize that gp17, after making the first cut, remains stably bound to the termini under physiological conditions and thus unable to make random cuts elsewhere in the genome. In fact, the λ terminase-end complex formed following

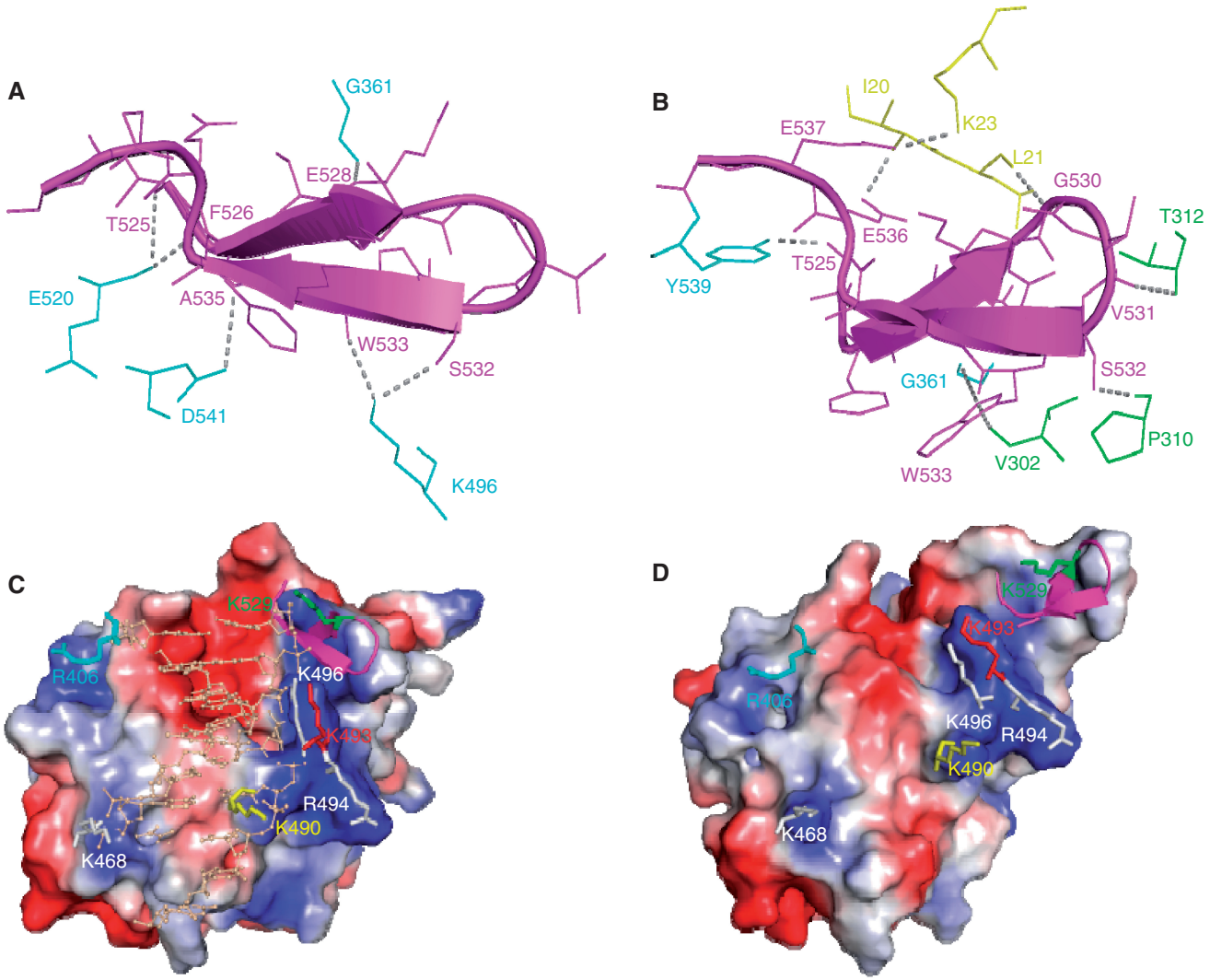

Figure 7. Networks of interactions in the tensed and relaxed states. (**A**) and (**B**): the position of β-hairpin (magenta) in tensed state (A) and relaxed state (B) is stabilized by networks of interactions with residues from ATPase subdomain I (green); subdomain II (yellow) and nuclease domain (cyan). The β-hairpin residues are shown in magenta. (**C**) and (**D**) Surface views of the DNA binding groove of tensed state (C) and relaxed state (D). The residues R406, K468, K490, K493, R494, K496 and K529 lining the groove are shown. Surface view is colored according to charge (blue, basic residues; red, acidic residues; white, neutral residues). The β-hairpin is shown as magenta ribbon and the DNA binding residues are shown as sticks. The residues that change positions significantly when gp17 interconverts between tensed and relaxed states are shown in color (R406, cyan; K490, yellow; K493, red; K529, green), and the residues that do not significantly change positions are shown in white (K468, R494 and K496). The DNA groove of the tensed state has the basic residues aligned with the phosphates of the modeled DNA, whereas the groove of the relaxed state is narrower, has less overall positive charge, and some of the residues moved away relative to the DNA-phosphates.

cutting at *cosN* is shown to be a highly stable complex with a long half-life, ~8 h (44).

ATP stimulates gp17 nuclease activity. At 1–2 mM ATP, nearly all the added DNA was degraded to very short DNA fragments. The non-hydrolyzable analogs, ATPγS or AMP-PNP, at best showed low level of stimulation, suggesting that hydrolysis of ATP, not just binding, is important for maximal stimulation. Consistent with this hypothesis, gp16, which greatly stimulates ATP hydrolysis of the N-terminal ATPase domain, showed the strongest stimulation. Several lines of evidence argue that the observed stimulation was not due to direct input of ATP energy into cutting but due to conformational changes induced in the ATPase domain by ATP hydrolysis, which modulate the nuclease center. First, cutting by gp17 *per se* does not require ATP energy, which is also true for other large terminases from phages λ and SPP1 (11,45,46). Second, there is no structural or biochemical evidence for a canonical ATP binding site near the nuclease catalytic site or elsewhere in the C-domain. Moreover, the nuclease activity of the isolated C-domain is approximately 13 times lower than the full-length protein (23), and it was not stimulated by ATP, suggesting that its linkage to the ATPase domain is important for catalysis as well as regulation. Third gp16, in the absence of ATP, nearly completely inhibits the nuclease activity of the full-length gp17 (26), but not of the isolated C-domain (data not shown).

Thus it is clear from our biochemical results that there is communication between the domains, and conformational changes triggered by the nucleotide-state of the ATPase center regulate nuclease function. The structural elements that link the ATPase and nuclease domains therefore must play a critical role in relaying the conformational signals. X-ray structures (22) show that the interdomain link consists of three basic parts: residues of ATPase subdomain II (amino acids 1–58 and amino acids 314–353), a linker or hinge (amino acids 354–364) and a β-hairpin from the C-domain (amino acids 525–535). Does the β-hairpin act as a chief regulator, as proposed by Smits *et al.* (24)? The β-hairpin of the phage SPP1 C-domain is thought to adopt two conformational states, nuclease active and inactive (24). The inherent flexibility of the β-hairpin, which is uniquely present in phage terminases but lacking in homologous nucleases such as RNase Hs, resolvases and intergrases, allows it to either move away from the nuclease DNA groove (nuclease active conformation) or clash with the DNA bound in the groove (nuclease inactive conformation). Indeed, the crystal structure of gp17 C-domain of T4 related phage RB49 shows no density at the β-hairpin region, whereas the T4 C-domain structural model shows a disordered loop that clashes with the bound DNA and the full-length gp17 structure shows a β-hairpin at the same position (22,23) (Supplementary Figure S2). The recently reported herpesvirus nuclease domain structure also shows no density at the same position (25). Furthermore, normal mode analysis of the T4 nuclease domain shows that the disordered loop moves into or away from the DNA binding groove, similar to the motion suggested for SPP1 nuclease (Supplementary Movie S1).

We however found that the above model can only be plausible in the context of the isolated nuclease domain. But in the full-length gp17, where the C-terminal nuclease domain is linked to the N-terminal ATPase domain via a flexible hinge, normal mode analysis does not show a dramatic movement of the β-hairpin, but rather a rigid body motion of the nuclease domain centered at the interdomain hinge, similar to that proposed in our translocation mechanism (22) (Supplementary Movie S2).

Comparison of the tensed and relaxed conformational states of gp17 further show that β-hairpin movement does not clash with the bound DNA in either state. In fact in the relaxed state, the β-hairpin moves away from the DNA groove and forms new contacts with the ATPase subdomains I and II (Figure 7B). On the other hand, the topology of the putative DNA binding residues is different in the relaxed and tensed states. In the tensed state, K529 (β-hairpin residue) and the other four positive residues, K490, K493, R494 and K496, that line one side of the nuclease groove are ~21–23Å from R406 or K468 that line the other side of the groove (Figure 7C). In tensed state, these residues would be able to position the ~23Å wide DNA in the groove for cutting. In the relaxed state however, K529 is predicted to move ~5Å away while the four positive residues move ~4Å closer to R406, 'compressing' the DNA groove (Figure 7D), and may not be able to correctly position the DNA for cutting. The orientation of the catalytic triad residues (D401, E458 and D542) do not, however, change from the tensed to the relaxed state (Supplementary Figure S1). These structural analyses predict that alterations in the topology of DNA binding residues, not clashing of the β-hairpin with bound DNA, is what is important for nuclease regulation, the tensed state being the most active and the relaxed state being the least active.

Conformational switching between tensed and relaxed states is controlled, at least in part, by the nucleotide state of the N-terminal ATPase center (22,26). Since the tensed state is the ATP bound state, our biochemical results showing nuclease stimulation under high turnover of ATP hydrolysis, i.e. in the presence of gp17, gp16 and ATP, are consistent with the structural analyses. Other regulators such as high salt may neutralize the interdomain charge pairs favoring the relaxed or nuclease inactive state whereas low concentrations will have the opposite effect, as has been observed experimentally. Similarly, gp16 interaction with the ATPase domain in the absence of ATP might favor the relaxed state, inhibiting cutting. Some of the previous observations are also consistent with this model. These include lack of nuclease activity in a chitin-intein purified gp17 (6), which was probably due to stabilization of gp17 in the relaxed state. The preferential cutting of transcriptionally active DNA (18) and regaining of cutting activity by the chitin-intein purified gp17 in the presence of gp16, ATP and T4 transcriptional factors (32) might be due to attainment of nuclease-active tensed state.

The above biochemical and structural analyses imply that one of the mechanisms by which the headful nuclease is regulated is by interdomain communication. We suggest, based on the current knowledge, that a 'communication track' consisting of residues from subdomain II, hinge and β-hairpin relays conformational signals from the ATPase center to the nuclease center. Different networks of interactions form when the protein interconverts between tensed and relaxed states (Figure 7A and B), remodeling the nuclease groove into active or inactive states. As our previous studies showed, this track is also fundamentally important for driving DNA movement and is highly sensitive to mutation. For example, the T287A mutation in the ATPase coupling motif, or the W533A mutation in the β-hairpin, show complete loss of cutting as well as translocation activities (22,47), perhaps due to the loss of key interactions involved in the relay process. In other words, the mutant proteins might be 'permanently' stuck in the relaxed state, unable to carry out either translocation or cutting.

Finally, our analyses lead to a model for the coupling of DNA cutting to packaging. In the infected cell where both gp16 and ATP are present, the gp17-nuclease would be in the stimulated (tensed) state forming a holo-terminase complex and efficiently cutting the concatemer (first cut) (Figure 5D). The terminase remains bound to the end, as has been observed at physiological concentrations of Mg and NaCl (Figure 8A). The terminase-DNA complex then docks onto prohead portal and initiates packaging. This is evidently a fast event, occurring on the order of seconds (7), thereby channeling the complex to translocation

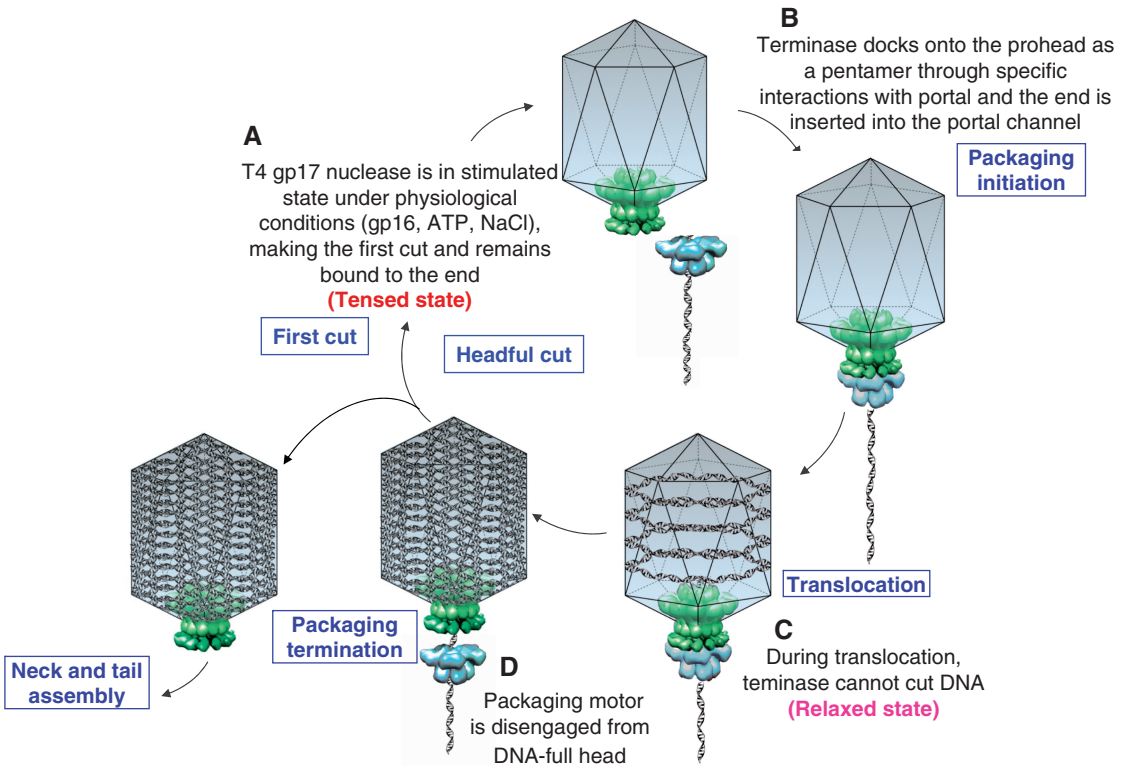

Figure 8. A model for coupling DNA cutting to DNA packaging. gp17 (blue) is shown as a pentamer, portal (green) as a dodecamer inserted at the special vertex of the icosahedral capsid, and DNA as a grey ribbon. In the presence of gp16, gp17 and ATP, a stimulated holo-terminase complex (tensed state) makes the first cut (**A**). The terminase-DNA complex then docks onto prohead portal as a pentamer and initiates packaging (**B**). During active translocation (**C**), gp17 is incompetent for cutting (relaxed state). After headful packaging, the packaging motor dissociates (**D**), re-forms holo-terminase complex (tensed state), and makes the headful cut. The terminase-DNA complex once again docks onto the portal of another empty prohead, initiating another round of genome packaging. The stoichiometry of the holo-terminase complexes that makes the first cut or the headful cut is unknown. See 'Discussion' section for additional details.

rather than non-specific fragmentation of the genome (Figure 8B) (23,31). During active translocation (Figure 8C), gp17 is mostly in the relaxed (nuclease inactive) state although tensed state does appear, but only transiently [~1 ms in each translocation cycle (7,22)]. Other factors; fast translocation rate (up to 2000 bp/sec), nuclease groove facing away from the translocating DNA, and requirement to form an anti-parallel dimer, also render the nuclease essentially incompetent for cutting during translocation. After encapsidation of a headful genome, a combination of factors; stalling of packaging (48), internal pressure from the packed DNA (48), structural changes in the portal (49) and assembly of neck proteins (50), disengage the packaging motor from the portal (Figure 8D). The freed gp17 subunits in association with gp16 and possibly with additional free gp17 subunits re-form the nuclease-active complex (tensed state) and make the termination cut (headful cut). The terminase-DNA complex still bound to the newly generated end then docks onto the portal of another empty prohead, initiating another round of genome packaging.

Thus, the packaging motor undergoes dynamic remodeling during processive packaging, interconverting between cutting and translocation states. Although the pentamer stoichiometry of the motor in the translocation state has been well established, the stoichiometry of the terminase complex in the cutting state is unknown. The latter might also differ between the complexes that make the first cut versus the headful cut. Also unknown is the precise role of portal in headful cutting, whether the portal conformational changes following head filling cause disengagement of the motor or signal gp17 to cut DNA. Another puzzling question is how the cleaved DNA in the nuclease groove 'transmigrates' to the translocation groove located on another face of the C-domain. Biochemical analyses and crystallization of terminase complexes are being pursued to address these basic questions. Nevertheless, our studies show that the mechanism and frequency of cutting, and coupling between cutting and packaging, are governed, at least in part, by the unique catalytic and regulatory properties of the headful nuclease. In particular, regulation of catalysis of the nuclease domain by the packaging ATPase domain via an interdomain communication relay is a novel mechanism that to our knowledge has not been observed in any other nucleases.

SUPPLEMENTARY DATA

Supplementary Data are available at NAR Online.

ACKNOWLEDGEMENTS

We thank Drs Michael Rossmann and Siyang Sun (Purdue University) and Kiran Kondabagilu (Catholic University) for stimulating discussions throughout this investigation and critical review of the article; graduate students Ms Danielle Chandler and Mr David Wells (University of Illinois) for help with molecular dynamics simulations.

FUNDING

Funding for open access charge: National Science Foundation (MCB-0923873); National Institutes of Health (NIBIB-EB009869-01 to V.B.R.).

Conflict of interest statement. None declared.

REFERENCES

1. Hendrix,R.W. (2002) Bacteriophages: evolution of the majority. *Theor. Popul. Biol.*, **61**, 471–480.
2. Mosig,G. (1987) The essential role of recombination in phage T4 growth. *Ann. Rev. Gen.*, **21**, 347–371.
3. Mosig,G. and Eiserling,F.A. (2004) T4 and Related Phages: Structure and Development. In Calender,R. (ed.), *The Bacteriophages*, 2nd edn. Oxford University Press, London.
4. Rao,V.B. and Feiss,M. (2008) The bacteriophage DNA packaging motor. *Annu. Rev. Genet.*, **42**, 647–681.
5. Leffers,G. and Rao,V.B. (2000) Biochemical characterization of an ATPase activity associated with the large packaging subunit gp17 from bacteriophage T4. *J. Biol. Chem.*, **275**, 37127–37136.
6. Baumann,R.G. and Black,L.W. (2003) Isolation and characterization of T4 bacteriophage gp17 terminase, a large subunit multimer with enhanced ATPase activity. *J. Biol. Chem.*, **278**, 4618–4627.
7. Fuller,D.N., Raymer,D.M., Kottadiel,V.I., Rao,V.B. and Smith,D.E. (2007) Single phage T4 DNA packaging motors exhibit large force generation, high velocity, and dynamic variability. *Proc. Natl Acad. Sci. USA*, **104**, 16868–16873.
8. Catalano,C.E., Cue,D. and Feiss,M. (1995) Virus DNA packaging: the strategy used by phage lambda. *Mol. Microbiol.*, **16**, 1075–1086.
9. Cue,D. and Feiss,M. (1997) Genetic evidence that recognition of cosQ, the signal for termination of phage lambda DNA packaging, depends on the extent of head filling. *Genetics*, **147**, 7–17.
10. Bravo,A., Alonso,J.C. and Trautner,T.A. (1990) Functional analysis of the *bacillus subtilis* bacteriophage SPP1 pac site. *Nucleic Acids Res.*, **18**, 2881–2886.
11. Camacho,A.G., Gual,A., Lurz,R., Tavares,P. and Alonso,J.C. (2003) *Bacillus subtilis* bacteriophage SPP1 DNA packaging motor requires terminase and portal proteins. *J. Biol. Chem.*, **278**, 23251–23259.
12. Casjens,S. and Weigele,P. (2005) Headful DNA Packaging by Bacteriophage P22. In Catalano,C. (ed.), *Viral Genome Packaging Machines: Genetics, Structure and Mechanism*. Landes Publishing, Georgetown, TX, pp. 80–88.
13. Rao,V.B. and Black,L.W. (2005) DNA Packaging in Bacteriophage T4. In Catalano,C. (ed.), *Viral Genome Packaging Machines: Genetics, Structure and Mechanism*. Landes Biosciences, Georgetown, Texas, pp. 40–58.
14. Lin,H. and Black,L.W. (1998) DNA requirements in vivo for phage T4 packaging. *Virology*, **242**, 118–127.
15. Rao,V.B. and Black,L.W. (1988) Cloning, overexpression and purification of the terminase proteins gp16 and gp17 of bacteriophage T4: construction of a defined in vitro DNA packaging system using purified terminase proteins. *J. Mol. Biol.*, **200**, 475–488.
16. Rao,V.B. and Mitchell,M.S. (2001) The N-terminal ATPase site in the large terminase protein gp17 is critically required for DNA packaging in bacteriophage T4. *J. Mol. Biol.*, **314**, 401–411.
17. Mitchell,M.S., Matsuzaki,S., Shosuke,I. and Rao,V.B. (2002) Sequence analysis of bacteriophage T4 DNA packaging/terminase genes 16 and 17 reveals a common ATPase center in the large subunit of viral terminases. *Nucleic Acids Res.*, **30**, 4009–4021.
18. Bhattacharyya,S.P. and Rao,V.B. (1993) A novel terminase activity associated with the DNA packaging protein gp17 of bacteriophage T4. *Virology*, **196**, 34–44.
19. Kuebler,D. and Rao,V.B. (1998) Functional analysis of the DNA-packaging/terminase protein gp17 from bacteriophage T4. *J. Mol. Biol.*, **281**, 803–814.
20. Rentas,F.J. and Rao,V.B. (2003) Defining the bacteriophage T4 DNA packaging machine: evidence for a C-terminal DNA cleavage domain in the large terminase/packaging protein gp17. *J. Mol. Biol.*, **334**, 37–52.
21. Sun,S., Kondabagil,K., Gentz,P.M., Rossmann,M.G. and Rao,V.B. (2007) The structure of the ATPase that powers DNA packaging into bacteriophage T4 procapsids. *Mol. Cell.*, **25**, 943–949.
22. Sun,S., Kondabagil,K., Draper,B., Alam,T.I., Bowman,V.D., Zhang,Z., Hegde,S., Fokine,A., Rossmann,M.G. and Rao,V.B. (2008) The structure of the phage T4 DNA packaging motor suggests a mechanism dependent on electrostatic forces. *Cell*, **135**, 1251–1262.
23. Alam,T.I., Draper,B., Kondabagil,K., Rentas,F.J., Ghosh-Kumar,M., Sun,S., Rossmann,M.G. and Rao,V.B. (2008) The headful packaging nuclease of bacteriophage T4. *Mol. Microbiol.*, **69**, 1180–1190.
24. Smits,C., Chechik,M., Kovalevskiy,O.V., Shevtsov,M.B., Foster,A.W., Alonso,J.C. and Antson,A.A. (2009) Structural basis for the nuclease activity of a bacteriophage large terminase. *EMBO Rep.*, **10**, 592–598.
25. Nadal,M., Mas,P.J., Blanco,A.G., Arnan,C., Solà,M., Hart,D.J. and Coll,M. (2010) Structure and inhibition of herpesvirus DNA packaging terminase nuclease domain. *Proc. Natl Acad. Sci. USA*, **107**, 16078–16083.
26. Al-Zharani,A.S., Kondabagil,K., Gao,S., Kelly,N., Ghosh-Kumar,M. and Rao,V.B. (2009) The small terminase, gp16, of Bacteriophage T4 is a regulator of the DNA packaging motor. *J. Biol. Chem.*, **284**, 24490–24500.
27. Goldberg,E., Grinius,L. and Letellier,L. (1994) Recognition, attachment, and injection. In Karam,J.D. (ed.), *Molecular Biology of Bacteriophage T4*. American Society for Microbiology, Washington, DC, pp. 347–356.
28. Pierce,J.C., Sauer,B. and Sternberg,N. (1992) A positive selection vector for cloning high molecular weight DNA by the bacteriophage P1 system: Improved cloning efficacy. *Proc. Natl Acad. Sci. USA*, **89**, 2056–2060.
29. Phillips,J.C., Braun,R., Wang,W., Gumbart,J., Villa,E., Chipot,C., Skeel,R.D., Kale,L. and Schulten,K. (2005) Scalable molecular dynamics with NAMD. *J. Comput. Chem.*, **26**, 1781–1802.
30. Trabuco,L.G., Villa,E., Mitra,K., Frank,J. and Schulten,K. (2008) Flexible fitting of atomic structures into electron microscopy maps using molecular dynamics. *Structure*, **16**, 673–683.
31. Kondabagil,K.R., Zhang,Z.B. and Rao,V.B. (2006) The DNA translocation ATPase of Bacteriophage T4 packaging motor. *J. Mol. Biol.*, **363**, 786–799.
32. Black,L.W. and Peng,G. (2006) Mechanistic coupling of bacteriophage T4 DNA packaging to components of the replication-dependent late transcription machinery. *J. Biol. Chem.*, **281**, 25635–25643.
33. Louie,D. and Serwer,P. (1991) Effects of temperature on excluded volume-promoted cyclization and concatemerization of cohesive-ended DNA longer than 0.04 Mb. *Nucleic Acids Res.*, **19**, 3047–3054.
34. Kech,J.L., Goedken,E.R. and Marqusee,S. (1998) Activation/Attenuation Model for RNase H: a one metal mechanism with second-metal inhibition. *J. Biol. Chem.*, **273**, 34128–34133.
35. Nowotny,M. and Yang,W. (2006) Stepwise analyses of metal ions in RNase H catalysis from substrate destabilization to product release. *EMBO J.*, **25**, 1924–1933.

36. Yang,W., Lee,J.Y. and Nowotny,M. (2006) Making and breaking nucleic acids: two-Mg^{2+} ion catalysis and substrate specificity. *Mol. Cell.*, **22**, 5–13.
37. Ortega,M.E., Gaussier,H. and Catalano,C.E. (2007) The DNA maturation domain of gpA, the DNA packaging motor protein of bacteriophage lambda, contains an ATPase site associated with endonuclease activity. *J. Mol. Biol.*, **373**, 851–865.
38. Wu,D.G. and Black,L.W. (1987) Gene amplification mechanism for the hyperproduction of T4 bacteriophage gene 17 and 18 proteins. *J. Mol. Biol.*, **195**, 769–783.
39. Vanamee,E.S., Santagata,S. and Aggarwal,A.K. (2001) FokI requires two specific DNA sites for cleavage. *J. Mol. Biol.*, **309**, 69–78.
40. Pingoud,A., Fuxreiter,M., Pingoud,V. and Wende,W. (2005) Type II restriction endonucleases: structure and mechanism. *Cell. Mol. Life Sci.*, **62**, 685–707.
41. Xin,W. and Feiss,M. (1993) Function of IHF in lambda DNA packaging: I. Identification of the strong binding site for integration host factor and the locus for intrinsic bending in cosB. *J. Mol. Biol.*, **230**, 492–504.
42. Ortega,M.E. and Catalano,C.E. (2006) Bacteriophage lambda gpNu1 and *Escherichia coli* IHF proteins cooperatively bind and bend viral DNA: implications for the assembly of a genome packaging motor. *Biochemistry*, **45**, 5180–5189.
43. Neaves,K.J., Cooper,L.P., White,J.H., Carnally,S.M., Dryden,D.T.F., Edwardson,J.M. and Henderson,R.M. (2009) Atomic Force Microscopy of the EcoKI Type-I DNA restriction enzyme bound to DNA shows enzyme dimerization and DNA looping. *Nucleic Acids Res.*, **37**, 62053–62063.
44. Yang,Q., Hanagan,A. and Catalano,C.E. (1997) Assembly of a Nucleoprotein complex required for DNA packaging by bacteriophage lambda. *Biochemisry*, **36**, 2744–2752.
45. Gual,A., Camacho,A.G. and Alonso,J.C. (2000) Functional analysis of the terminase large subunit, G2P, of *Bacillus subtilis* bacteriophage SPP1. *J. Biol. Chem.*, **275**, 35311–35319.
46. Feiss,M. and Catalano,C.E. (2005) Bacteriophage Lambda Terminase and the Mechanism of Viral DNA Packaging. In Catalano,C. (ed.), *Viral Genome Packaging*. Landes Biosciences, Georgetown, Texas, pp. 40–58.
47. Draper,B. and Rao,V.B. (2007) An ATP hydrolysis sensor in the DNA packaging motor from bacteriophage T4 suggests an inchworm-type translocation mechanism. *J. Mol. Biol.*, **369**, 79–94.
48. Smith,D.E., Tans,S.J., Smith,S.B., Grimes,S., Anderson,D.L. and Bustamante,C. (2001) The bacteriophage straight phi29 portal motor can package DNA against a large internal force. *Nature*, **413**, 748–752.
49. Lander,G.C., Tang,L., Casjens,S.R., Gilcrease,E.B., Pervelige,P., Poliakov,A., Potter,C.S., Carragher,B. and Johnson,J.E. (2006) The structure of an infectious P22 virion shows the signal for headful DNA packaging. *Science*, **312**, 1791–1795.
50. Zheng,H., Olia,A.S., Gonen,M., Andrews,S., Cingolani,G. and Gonen,T. (2008) A conformational switch in bacteriophage p22 portal protein primes genome injection. *Mol. Cell.*, **29**, 376–383.